PHYSICAL REVIEW B **96**, 205442 (2017)

Interacting Majorana chain: Transport properties and signatures of an emergent two-dimensional weak topological phase

Zhao Liu,[1] Emil J. Bergholtz,[2] Alessandro Romito,[3] and Dganit Meidan[4]
[1]*Dahlem Center for Complex Quantum Systems and Institut fur Theoretische Physik, Freie Universitat Berlin, 14195 Berlin, Germany*
[2]*Department of Physics, Stockholm University, AlbaNova University Center, 106 91 Stockholm, Sweden*
[3]*Department of Physics, Lancaster University, Lancaster LA1 4YB, United Kingdom*
[4]*Department of Physics, Ben-Gurion University of the Negev, Beer-Sheva 84105, Israel*
(Received 11 July 2017; published 28 November 2017)

We study a one-dimensional chain of $2N$ Majorana bound states, which interact through a local quartic interaction. This model describes for example the edge physics of a quasi-one-dimensional (1D) stack of $2N$ Kitaev chains with modified time-reversal symmetry $T\gamma_i T^{-1} = \gamma_i$, which precludes the presence of quadratic coupling. The ground state of our 1D Majorana chain displays a fourfold periodicity in N, corresponding to the four distinct topological classes of the stacked Kitaev chains. We analyze the transport properties of the 1D Majorana chain, when probed by local conductors located at its ends. We find that for finite but large N, the scattering matrix partially reflects the fourfold periodicity, and the chain exhibits strikingly different transport properties for different chain lengths. In the thermodynamic limit, the 1D Majorana chain hosts a robust many-body zero mode, which indicates that the corresponding stacked two-dimensional bulk system realizes a weak topological phase.

DOI: 10.1103/PhysRevB.96.205442

I. INTRODUCTION

Models of interacting Majorana modes provide a simple platform to study novel physical phenomena. Examples range from emergent supersymmetric quantum critical behavior [1] to the physics of black holes [2,3]. One particularly interesting example is the Sachdev-Ye-Kitaev (SYK) model with random all-to-all Majorana interactions [2,3], which is a calculable model with implications for quantum gravity, quantum information, and quantum chaos [3–15]. Recent proposals for the realization of the SYK model would potentially allow to experimentally probe this physics in a solid state setup [12,16]. A variant of the SYK model with strong short-range interactions was suggested to exhibit emergent supersymmetric quantum critical behavior [1,17,18]. Interestingly, this short-range model describes excitations on the edge of stacked topological superconducting wires, which is potentially easier to access experimentally.

From a topological point of view, interactions are known to alter the topological classification of gapped phases as well as the nature of their emergent boundary states. By enlarging the phase space, interactions can connect otherwise distinct topological phases and reduce the number of gapped phases [19–23]. One notable example occurs in the stack of one-dimensional topological superconductors with a modified time-reversal symmetry $T^2 = 1$, corresponding to class BDI. Here the noninteracting system is characterized by a $\mathbb{Z}$ index which counts the number of Majorana modes at its boundary, while interactions reduce the number of gapped phases to eight (labeled by a $\mathbb{Z}_8$ topological index) [19].

It is conceptually useful to think of the eight topological subclasses as constructed by stacking L topological superconducting chains forming a slab of finite transverse size L [24], with L Majorana modes localized at its boundary. Interactions of finite range can gap the Majorana modes without breaking time-reversal symmetry if L is a multiple of eight, making a system of $L \mod 8 = 0$ topological superconducting chains adiabatically connected to a trivial insulator [19]. The remaining nontrivial phases host a spinless fermion, a Majorana quasiparticle, and a Kramers doublet, respectively, as boundary excitations. Each of these physical excitations have markedly distinct measurable features which can be detected when coupling the edge of the stacked system to external leads.

Indeed, transport properties provide a prominent tool to probe topological phases and the nature of their boundary states in (quasi-) one-dimensional systems [25,26]. The presence of gapless modes confined to the system ends affects the scattering of noninteracting fermions when the system is connected to leads. For noninteracting fermions in a quasi-1D wire, topological invariants of the system can be directly related to scattering matrix invariants [27,28], and measurable transport properties have been computed [26], also in the presence of disorder [29]. In fact, conductance measurements have been the first indications of possible topological phases in engineered nanostructures [30–33]. Remarkably, the nature of the boundary states that appear in the stacked BDI system allows to formulate the topological index using a scattering matrix approach—even in the presence of interactions [34,35].

As long as the number of stacked superconducting chains is kept finite, the $\mathbb{Z}_8$ periodicity of the system, being a topological property, persists independently of the detailed interaction profile. The interaction range, however, introduces a transverse length scale for the stacked quasi-1D system. When the interaction range scales with the system size, the boundary is essentially a zero-dimensional dot, resulting for example in the Sachdev-Ye-Kitaev model [2,3]. For a finite-size boundary, the $\mathbb{Z}_8$ periodicity of the system has been shown to emerge in the energy level statistics for random interaction strengths [6]. In the opposite limit when interactions are short ranged, the stacked setup is two dimensional (2D) of finite transverse size, with a 1D boundary. This setup allows us to analyze the nature of interacting 2D BDI system in the thermodynamic limit as

well as to study the transport properties *along* its 1D boundary, in order to determine which, if any, of the $\mathbb{Z}_8$ periodic structure persists when the boundary system is macroscopically large.

We study the transport properties along a 1D Majorana chain with local translationally invariant interactions in a setup where local leads are contacted to its two ends. [Equation (1) is the simplest generalization of the Hubbard model with Majorna degrees of freedom.] The model provides an effective description of the edge of stacked topological superconducting chains with modified time-reversal symmetry $T^2 = 1$, and has been shown to posses a rich phase diagram [1,17,18]. We restrict ourselves to an even number of Majorana fermions $L = 2N$ in the 1D chain, so that the corresponding stacked system consists of fermion excitations localized at a single edge of the 2D system, and falls into four distinct topological classes depending on $N \mod 4$. The nontrivial phases are known to host protected boundary excitations which can be detected when coupling the edge of the stacked system to external leads.

We compute the the scattering matrix of the 1D Majorana chain. Using the symmetries of the model, we show that the scattering matrix partially reflects the fourfold periodicity of the 2D bulk system, even when the chain is macroscopically large. The different phases of the stacked system are characterized by different scattering properties along the 1D Majorana chain on the boundary, which can be detected in transport measurements. We find that electrons scattered from the leads can be fully reflected, can acquire a π phase shift upon reflection, or can be transmitted across the chain, depending on the fourfold periodicity of $N \mod 4$. Though these distinct transport properties do not fully distinguish all different topological phases, their combination with the quantum dimension of the system's state [36], leads to a full classification of the different topological phases.

Our analysis shows that in the thermodynamic limit our 1D Majorana chain has a twofold degenerate ground state. The presence of this zero mode is stable for a generic interactions which do not break time-reversal and translational symmetry. Regarding the 1D Majorana chain as an effective model that emerges on the edge of stacked superconducting chains, the presence of a robust zero mode at $N \to \infty$ indicates that the two-dimensional bulk system is in a weak interacting topological phase, i.e., a topological phase protected by translational symmetry. This is quite remarkable given that its noninteracting analog is topologically trivial. Despite its stability, we show that the transport properties of the boundary zero mode become progressively harder to detect when the system is coupled to single channel leads. This is due to the fact that the tunneling matrix elements between the two degenerate ground states decay rapidly in the large N limit.

While the scattering properties along the Majorana chain of finite size are expected to depend on the detailed coupling to the leads and the form of interactions, generic local probes can distinguish a gapped system ($\nu = 0$), a fermionic zero-energy excitation ($\nu = 1$, $\nu = 3$), and a spin-1/2-like excitation ($\nu = 2$). Here $\nu = N \mod 4$ is the topological index. In addition, the properties of the system in the thermodynamic limit do not depend on the detailed coupling, and the weak topological phase is robust for a generic interaction profile which does not break translational invariance.

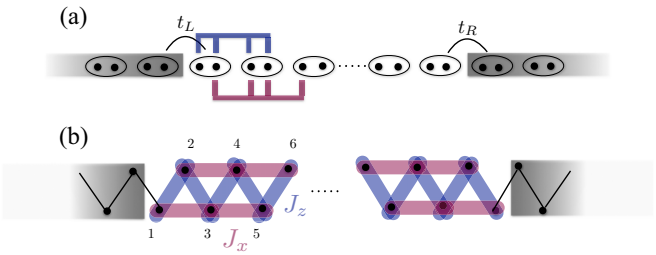

FIG. 1. (a) Schematics of a 1D chain of Majorana bound states coupled to left and right leads. Circled pairs of Majorana zero modes indicate fermionic degrees of freedom and colored lines represent different possible interaction terms. (b) Equivalent representation of the Majorana chain in (a) after its mapping to a spin model. The different interaction terms in (a) are represented by different spin coupling terms in (b) with the same color code.

II. MODEL AND SYMMETRIES

We study a 1D Majorana chain of length $L = 2N$ with short-range interactions under open boundary conditions, as described by the Hamiltonian

$$H_0 = -W \sum_{i=1}^{2N-3} \gamma_i \gamma_{i+1} \gamma_{i+2} \gamma_{i+3}, \tag{1}$$

where γ_j are Majorana bound state operators defined by the algebra $\{\gamma_j, \gamma_k\} = 2\delta_{j,k}$ and $\gamma_j = \gamma_j^\dagger$. The system is sketched in Fig. 1(a). This 1D chain describes for example the low-energy physics on the edge of a quasi-1D system composed of $2N$ Kitaev chains [24] with modified time-reversal symmetry $T \gamma_i T^{-1} = \gamma_i$ (symmetry class BDI) [37–39], which precludes the presence of quadratic Majorana terms [19].

Note that, following a Jordan-Wigner transformation, the Hamiltonian (1) can be expressed in terms of spin degrees of freedom as

$$H_0 = W \sum_{i=1}^{N-1} \sigma_i^z \sigma_{i+1}^z + W \sum_{i=1}^{N-2} \sigma_i^x \sigma_{i+2}^x, \tag{2}$$

which has a natural interpretation in terms of the ladder spin-chain sketched in Fig. 1(b).

The model has three discrete symmetries. The first is a charge conjugation symmetry $H_0 = T_L H_0 T_L^{-1}$, which can be represented as

$$T_L = \begin{cases} \left[\prod_{j=1}^{N} \gamma_{2j-1}\right] K, & N \in \text{odd}, \\ \left[\prod_{j=1}^{N} \gamma_{2j}\right] K, & N \in \text{even}, \end{cases}$$

where K denotes complex conjugation. Regarding the chain as describing the edge model of a quasi-1D bulk composed of $2N$ Kitaev chains, this operator can be understood as the projection of the global time-reversal symmetry on the low-energy degrees of freedom on the edge [20,21]. Importantly, while the global time-reversal symmetry $T^2 = 1$, its local projection $T_L^2 = \pm 1$ depends on the total number of fermionic sites N of the chain. In addition to charge conjugate, the system possesses two additional symmetries, namely the parity of the odd or the

even subchain, respectively:

$$P_o = \prod_i (-i\gamma_{4i-3}\gamma_{4i-2}),$$

$$P_e = \prod_i (-i\gamma_{4i-1}\gamma_{4i}).$$

Studying the representations of the three discrete symmetries as a function of the number of spins N reveals that the Majorana chain described in Eq. (2) falls into four symmetry-protected topological phases labeled by different $\nu = N \mod 4$. Those are distinguished by the sign of T_L^2 and by the fact that time-reversal symmetry commutes or anticommutes with the total parity $P = P_o P_e$ [21,40]. In addition, for the Hamiltonian in Eq. (1), the four symmetry-protected phases can be characterized by different subsets of noncommuting symmetry operators:

(A) For a chain with $\nu = 0$, the local time-reversal operator commutes with both even chain and odd chain parities $[T_L, P_e] = [T_L, P_o] = 0$, and the system has a unique ground state.

(B) For a chain with $\nu = 1$, $\{T_L, P_o\} = 0$, giving rise to a twofold degeneracy of the ground-state manifold, where the two ground states differ by the parity of the odd chain.

(C) For a chain with $\nu = 2$, $\{T_L, P_o\} = \{T_L, P_e\} = 0$, and the ground state is twofold degenerate, where the two ground states differ by the relative parities of the odd and the even chain but have the same total parity.

(D) For a chain with $\nu = 3$, $\{T_L, P_e\} = 0$, and the ground state is twofold degenerate, where the two ground states differ by the parity of the even chain.

Thus each of the three nontrivial phases ($\nu = 1,2,3$) are characterized by a twofold degenerate ground state, which is spanned by the parity of the even and/or odd subchains (Fig. 2), in contrast to the unique ground state in the trivial phase ($\nu = 0$).

III. TRANSPORT AND SCATTERING PROCESSES

To study the transport properties of the Majorana chain in Eq. (1), we assume that it is coupled to noninteracting leads located at two ends of the system. We consider local tunneling so that electrons can tunnel from the lead to the end-fermionic site of the chain, as described by the Hamiltonian $H = H_0 + H_T + H_L + H_R$, where

$$H_T = \sum_k t_L c_{L,k}^\dagger d_L + t_R c_{R,k}^\dagger d_R + \text{H.c.} \tag{3}$$

and

$$H_{j=L,R} = \sum_k \epsilon_j(k) c_{j,k}^\dagger c_{j,k}.$$

Here $c_{j,k}$ annihilates an electron of energy $\epsilon_j(k)$ with momentum k in lead j, $d_L = (\gamma_1 + i\gamma_2)/2$, and $d_R = (\gamma_{2N-1} + i\gamma_{2N})/2$, where L,R label the left and right leads [Fig. 1(a)]. The current operator at the left lead is

$$\hat{I}_L = \partial_t \hat{N}_L = -i \sum_k t_L c_{L,k}^\dagger d_L + \text{H.c.}$$

In general, the evaluation of the average current $\langle I_{i=L,R} \rangle$ and the low frequency current fluctuations $\mathscr{S}_{ij\in\{L,R\}} = \mathscr{S}_{ij}(\omega=0) = \int dt \, \langle [I_i(t) - \langle I_i \rangle, I_j(0) - \langle I_j \rangle]_+ \rangle$ through the interacting system in Eq. (1) encompasses multiparticle as well as energy-nonconserving processes. However, at voltage biases and temperature lower than the gap that separates the ground-state manifold from the excited states, i.e., $eV_L, eV_R \ll \Delta_g$, the system is characterized either by a nondegenerate or by a doubly degenerate ground state. As we discuss in the detailed analysis below, in both cases, the low energy physic is described by a Fermi liquid and the transport properties can be fully characterized by a unitary scattering matrix $\Psi_{\text{out}} = \mathcal{S}\Psi_{\text{in}}$. The scattering states are in the basis $\Psi_{\text{in}} = [\psi_{L,e}(E), \psi_{L,h}(E), \psi_{R,e}(E), \psi_{R,h}(E)]^T$ of electron (e)

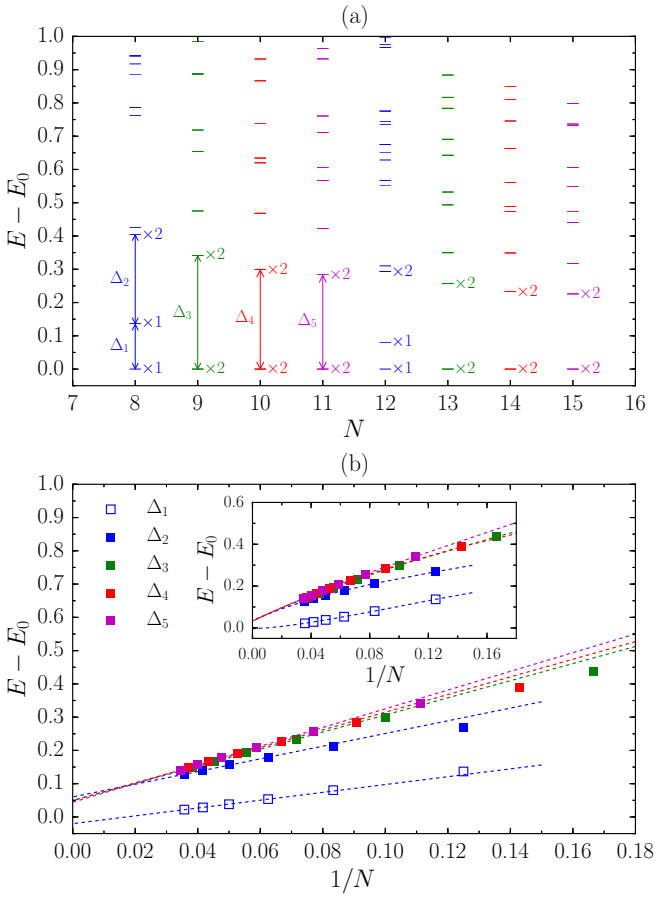

FIG. 2. (a) Typical many-body spectra for different system sizes $N = 8$–15. The degeneracies of some low-lying levels are indicated by the numbers nearby. For $N \mod 4 = 1,2,3$, all energy levels are exactly twofold degenerate. For $N \mod 4 = 0$, the lowest two levels are nondegenerate, while the third level is again exactly twofold degenerate. (b) The scaling of the low-energy gaps as defined in (a) with increasing system sizes up to $N = 29$. The linear fitting (dashed line) is made according to the data of the largest four system sizes for each $N \mod 4$. The negative y intercept for Δ_1 suggests that the twofold exact degeneracy of the lowest two levels for $N \mod 4 = 0$ will be recovered in the thermodynamic limit. The y intercepts for the other four gaps have roughly similar nonzero values, suggesting finite gaps in the thermodynamic limit. Intriguingly, as shown in the inset, the unique fifth order polynomial in $1/N$ that goes through all data points for each $N \mod 4$ gives a y intercept for Δ_1 remarkably close to zero while the $\Delta_{2,3,4,5}$'s extrapolate to virtually identical finite values. We set $W = 0.5$ in this figure.

and hole (h) modes at a given energy ϵ from the Fermi seas of the left and right leads.

At zero temperature the current at the left lead L and the current fluctuations can be expressed as [41–43]

$$I_L = \frac{e}{h} \sum_{a,b=e,h} \sum_{j=L,R} \mathrm{sgn}(a) \int dE\, \mathcal{A}_{jb;jb}(L,a;E) f_{j,b}(E), \tag{4}$$

$$\mathcal{S}_{ij} = \frac{2e^2}{h} \sum_{k,l=L,R} \sum_{a,b,\gamma,\delta=e,h} \mathrm{sgn}(a)\,\mathrm{sgn}(b) \times \int dE\, \mathcal{A}_{k\gamma;l\delta}(i,a;E) \mathcal{A}_{l\delta;k\gamma}(j,b;E) f_{k,\gamma}(E) \times [1 - f_{l,\delta}(E)], \tag{5}$$

where $\mathcal{A}_{k\gamma;l\delta}(i,a;E) = \delta_{i,k}\delta_{i,l}\delta_{a,\gamma}\delta_{a,\delta} - s^{a\gamma *}_{ik}(E) s^{a\delta}_{il}(E)$ with $s^{\delta\gamma}_{ik}$ the components of the scattering matrix $\mathcal{S}$, $f_{j,b}(E) = \Theta[E - \mathrm{sgn}(b) eV_j]$ is the zero temperature Fermi-Dirac distribution, and $\mathrm{sgn}(a)$ is positive (negative) for $a = e(h)$. In the following subsections we study the transport properties of the different topological phases.

A. $\nu = 0$

A chain with $N \mod 4 = 0$ realizes a trivial phase with a unique ground state (quantum dimension 1), separated from the excited stated by a finite gap Δ_g, as shown in Fig. 2. At low voltage $eV < \Delta_g$, the system resembles a trivial insulator and the scattering matrix is $\mathcal{S}(\omega) = \mathbb{1}_{4\times 4}$.

B. $\nu = 1$

A chain with $N \mod 4 = 1$ has two degenerate ground states (quantum dimension 2) which are distinguished by the parity of the odd subchain. The ground-state manifold is separated by a finite gap Δ_g from the rest of the spectrum (Fig. 2). We distinguish the two ground states by the odd chain parity quantum number $P_o|\mathrm{gs}_\pm\rangle = \pm|\mathrm{gs}_\pm\rangle$. For a chain with $N \mod 4 = 1$, tunneling to and from the two leads changes the parity of the odd subchain and therefore may toggle between the two ground states. When projecting onto the ground-state manifold, and to the lowest order in the tunneling $t_{L,R}$, the operators d_1 and d_N can be expressed as

$$\mathcal{P} d_1 \mathcal{P} = \alpha |\mathrm{gs}_+\rangle\langle \mathrm{gs}_-| + \beta |\mathrm{gs}_-\rangle\langle \mathrm{gs}_+| \equiv \alpha f^\dagger + \beta f, \tag{6}$$

$$\mathcal{P} d_N \mathcal{P} = \tilde{\alpha} |\mathrm{gs}_+\rangle\langle \mathrm{gs}_-| + \tilde{\beta} |\mathrm{gs}_-\rangle\langle \mathrm{gs}_+| \equiv \tilde{\alpha} f^\dagger + \tilde{\beta} f, \tag{7}$$

where $\mathcal{P} = \sum_{s=\pm} |\mathrm{gs}_s\rangle\langle \mathrm{gs}_s|$ is the projection operator on the ground-state manifold. Since the system possesses an inversion symmetry $\mathcal{I}$, $\mathcal{I}\boldsymbol{\sigma}_j\mathcal{I}^{-1} = \boldsymbol{\sigma}_{N+1-j}$, which can be written as $\mathcal{I} d_j \mathcal{I}^{-1} = (\prod_{i=1}^{N-j} d_i^\dagger d_i) d_{N+1-j}$ in terms of the fermions, the coefficients introduced in Eqs. (6) and (7) satisfy $\alpha = \tilde{\alpha}$ and $\beta = -\tilde{\beta}$. The scaling of matrix elements α and β with system size is shown in Fig. 3. While α and β are substantially different in magnitude for any system size leading to interesting consequences in transport, we expect them to decay exponentially with a common exponent as we elaborate on in Sec. IV.

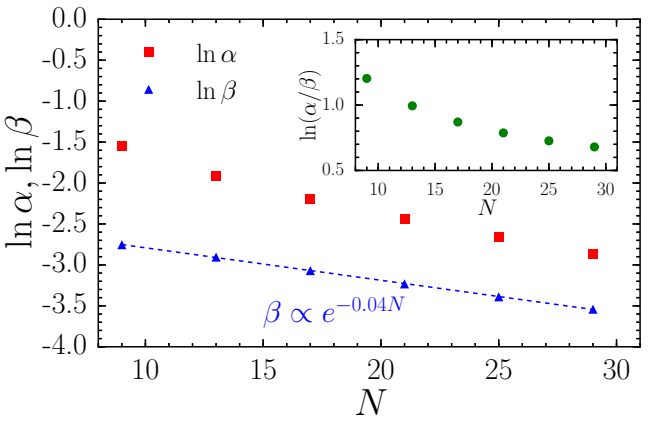

FIG. 3. The scaling of α and β with increasing system sizes for $N \mod 4 = 1$ up to $N = 29$. The exponential for $\beta \propto e^{-0.04N}$ is obtained by fitting (dashed line) the data of all system sizes. The precise scaling of α is harder to predict from the available system sizes, although it is most likely exponential in the large N limit. The inset shows the logarithm of the ratio α/β which likely approaches a finite value for large N, although the existing finite size data do not unambiguously confirm this scenario.

When projecting the Hamiltonian on the ground-state manifold, we find

$$\tilde{H} = \mathcal{P}(H_0 + H_T)\mathcal{P} = \mathcal{P} H_T \mathcal{P} = \sum_k \sum_{i=L,R} (\alpha_i c^\dagger_{i,k} f^\dagger + \beta_i c^\dagger_{i,k} f) + \mathrm{H.c.}, \tag{8}$$

where $\alpha_{L,R} = \alpha t_{L,R}$, $\beta_L = \beta t_L$, and $\beta_R = -\beta t_R$. Equation (8) shows that in the weak tunneling limit, the contributions to the current are dominated by single-particle processes. We can therefore compute the scattering matrix as

$$\mathcal{S}(\omega) = 1 - 2\pi i W^\dagger (\omega - \tilde{H} + i\pi W W^\dagger)^{-1} W,$$

where W is the matrix that describes the coupling of the ground-state manifold of Eq. (1) to the leads.

The resulting scattering matrix generically allows for all possible single-particle scattering channels which are controlled by the coupling to the leads and the interaction-dependent parameters α and β. When the leads are coupled symmetrically to the chain $t_L = t_R = t$, the scattering matrix takes a simple form:

$$\mathcal{S}(\omega) = \begin{pmatrix} s^{ee}_{LL} & s^{eh}_{LL} & s^{ee}_{LR} & 0 \\ s^{he}_{LL} & s^{hh}_{LL} & 0 & s^{hh}_{LR} \\ s^{ee}_{RL} & 0 & s^{ee}_{RR} & s^{eh}_{RR} \\ 0 & s^{hh}_{RL} & s^{he}_{RR} & s^{hh}_{RR} \end{pmatrix},$$

with

$$s^{ee}_{LL} = s^{hh}_{LL} = s^{ee}_{RR} = s^{hh}_{RR} = \frac{i\omega}{\Gamma(\alpha^2+\beta^2) + i\omega},$$

$$s^{ee}_{LR} = s^{ee}_{RL} = \frac{\Gamma(\beta^2 - \alpha^2)}{\Gamma(\alpha^2+\beta^2) + i\omega},$$

$$s^{he}_{LL} = s^{he}_{RR} = s^{eh}_{LL} = s^{eh}_{RR} = \frac{2\Gamma\alpha\beta}{\Gamma(\alpha^2+\beta^2) + i\omega},$$

and $\Gamma = 2\pi t^2$.

From Eq. (4) we obtain the current at the left lead

$$I_L = \frac{2e^2}{h}\left[V_L - V_R + \frac{4\alpha^2\beta^2}{(\alpha^2+\beta^2)^2}(V_L+V_R)\right].$$

Similarly, the zero-temperature noise is obtained from Eq. (5) as

$$\mathcal{S}_{LR}(\omega=0) = -\frac{2e^3}{h}\frac{[2\alpha\beta(\beta^2-\alpha^2)]^2}{(\alpha^2+\beta^2)^4}(V_L+V_R).$$

Note that $I_L \neq 0$ even when a voltage bias is applied only at one of the two leads. This is because electrons can be exchanged directly between the leads and the grounded bulk superconductor.

C. $\nu = 2$

For a chain with $N \mod 4 = 2$, the two degenerate ground states (quantum dimension 2) have opposite fermion parities on both the even and odd subchains. We label the two ground states as $|\mathrm{gs}_{+-}\rangle$ and $|\mathrm{gs}_{-+}\rangle$ where the two indices label the parity of the odd and even subchain, respectively, and we have assumed that the two ground states have odd total parity $P_e P_o$. Since H_T modifies the parity of only one of the two subchains, it has vanishing matrix elements on the ground-state manifold. Consequently, the low-voltage transport is dominated by virtual transition into the excited states.

To find how these higher order processes affect the transport properties, we perform a Schrieffer Wolff transformation to derive the effective Hamiltonian taking into account virtual transitions to excited states. The resulting effective model is up to an additive constant given by

$$\begin{aligned} H_{\mathrm{eff}} = &\sum_{j=L,R}\sum_k \epsilon_j(k) c^\dagger_{j,k}c_{j,k} + \frac{\tau_z}{2}\sum_{k,k'}\Big\{(J_z+\Delta_z) \\ &\times\left[c^\dagger_{Rk}c_{Rk'} - \frac{\delta_{k,k'}}{2}\right] - (J_z-\Delta_z)\left[c^\dagger_{Lk}c_{Lk'} - \frac{\delta_{k,k'}}{2}\right]\Big\} \\ &+\Big\{\tau_+\sum_{k,k'}\Big(J_- c^\dagger_{Rk}c_{Lk'} + J_+ c^\dagger_{Lk}c_{Rk'} \\ &+ \Delta_+ c^\dagger_{Lk}c^\dagger_{Rk'} + \Delta_- c_{Rk}c_{Lk'}\Big) + \mathrm{H.c.}\Big\}, \end{aligned} \tag{9}$$

where we have defined $\tau_z = |\mathrm{gs}_{+-}\rangle\langle\mathrm{gs}_{+-}| - |\mathrm{gs}_{-+}\rangle\langle\mathrm{gs}_{-+}|$ and $\tau_+ = |\mathrm{gs}_{+-}\rangle\langle\mathrm{gs}_{-+}|$, and the coefficients are given by

$$J_z = \sum_n \left\{|t_R|^2\frac{|\tilde\beta_n|^2 - |\tilde\alpha_n|^2}{E_g - E_n} - |t_L|^2\frac{|\beta_n|^2 - |\alpha_n|^2}{E_g - E_n}\right\},$$

$$J_- = 2t_R t_L^* \sum_n \frac{\tilde\beta_n \alpha_n^*}{E_g - E_n},$$

$$J_+ = 2t_R^* t_L \sum_n \frac{\tilde\alpha_n^* \beta_n}{E_g - E_n},$$

TABLE I. Values of the coefficients J_z, J_-, J_+, Δ_z, Δ_+, Δ_- entering the effective Hamiltonian Eq. (9) for different $N = 4m+2$.

	$N=10$	$N=14$	$N=18$
$J_z/(\lvert t_R\rvert^2+\lvert t_L\rvert^2)$	1.076385	1.071858	1.067348
$J_+/(2t_L t_R^*)$	0.420549	0.333439	0.27389
$J_-/(2t_L^* t_R)$	0.06542	0.0677778	0.0657269
$\Delta_z/(\lvert t_R\rvert^2-\lvert t_L\rvert^2)$	1.076385	1.071858	1.067348
$\Delta_+/(2t_L t_R)$	0.150967	0.141257	0.128129
$\Delta_-/(2t_L^* t_R^*)$	0.150967	0.141257	0.128129

and

$$\Delta_z = \sum_n \left\{|t_R|^2\frac{|\tilde\beta_n|^2 - |\tilde\alpha_n|^2}{E_g - E_n} + |t_L|^2\frac{|\beta_n|^2 - |\alpha_n|^2}{E_g - E_n}\right\},$$

$$\Delta_+ = 2t_R t_L \sum_n \frac{\tilde\beta_n \beta_n}{E_g - E_n},$$

$$\Delta_- = 2t_R^* t_L^* \sum_n \frac{\tilde\alpha_n^* \alpha_n^*}{E_g - E_n}.$$

Here the sum is over excited states $|n_{s,s'}\rangle$, for which $H_0|n_{s,s'}\rangle = E_n|n_{s,s'}\rangle$, $P_o|n_{s,s'}\rangle = s|n_{s,s'}\rangle$, and $P_e|n_{s,s'}\rangle = s'|n_{s,s'}\rangle$, E_g is the ground state and

$$\begin{aligned} \alpha_n &= \langle \mathrm{gs}_{-+}|d_1|n_{++}\rangle = (\langle \mathrm{gs}_{+-}|d_1^\dagger|n_{--}\rangle)^*, \\ \beta_n &= \langle \mathrm{gs}_{+-}|d_1|n_{--}\rangle = (\langle \mathrm{gs}_{-+}|d_1^\dagger|n_{++}\rangle)^*, \\ \tilde\alpha_n &= \langle \mathrm{gs}_{-+}|d_N|n_{--}\rangle = -(\langle \mathrm{gs}_{+-}|d_N^\dagger|n_{++}\rangle)^*, \\ \tilde\beta_n &= \langle \mathrm{gs}_{+-}|d_N|n_{++}\rangle = -(\langle \mathrm{gs}_{-+}|d_N^\dagger|n_{--}\rangle)^*, \end{aligned}$$

where the second equality follows from charge conjugation symmetry T_L. The symmetry of the system under spatial inversion $\mathcal{I}$, which for the case of $\nu = 2$ exchanges the even and odd parities ($P_e \leftrightarrow P_o$), imposes the constraints

$$\begin{aligned} \alpha_n &= \delta_n \tilde\beta_n, \\ \beta_n &= -\delta_n \tilde\alpha_n, \end{aligned}$$

where $\delta_n = \pm$ is an n-dependent sign. We evaluate α_n and β_n numerically for different system sizes and determine the corresponding values for the coefficients of the effective Hamiltonian J_z, J_-, J_+, Δ_z, Δ_+, Δ_-, which are reported in Table I.

The model described by Eq. (9) is a variant of the compactified two-channel Kondo model whose low-energy physics has been analyzed by the study of RG flow [35,44,45]. This analysis shows that the low voltage and temperature limit is governed by screening of the ground-state spin degree-of-freedom by the lead electrons, and the physics is that of a one-channel Kondo. At low temperature the system is described by a Fermi liquid theory and is characterized by a unitary scattering matrix which takes the standard form $\mathcal{S} = -\mathbb{1}_{4\times4}$ [46]. While this π phase shift does not affect the conductance, it can in principle be detected in a phase sensitive interference type of measurement. Importantly, the form of the scattering matrix is a direct consequence of the presence of two single-channel terminals, of the fact that a tunneling process cannot induce first order transitions within

the twofold degenerate ground state, and that these transition are generically present as second order process, as captured by (9).

D. $\nu = 3$

A chain with $N \mod 4 = 3$ is topological equivalent to a chain with $N \mod 4 = -1$, which is the inverse phase of $N \mod 4 = 1$ [34]. Here ν and $-\nu$ are inverse of each other in the sense that when combined, the phase and its inverse form a trivial phase [47]. The properties of two chains with $N \mod 4 = -1$ and $N \mod 4 = 1$ strongly resemble each other. Both phases are characterized by a twofold ground-state degeneracy (quantum dimension 2), and a fermionic zero mode that toggles between them, changing the total parity of the chain. In addition, a recent study of the energy level statistics in a related model with random long-range interactions [6] showed that the phase $\nu = 1$ and its inverse $\nu = -1$ have identical energy level statistics. Despite these similarities, our model with local interactions presents distinct transport properties for the two phases.

When $N \mod 4 = -1$, the ground-state manifold is spanned by the parity of the even subchain, while tunneling events from the left and right leads change the parity of the odd subchain. Therefore, tunneling of electrons to and from the leads does not introduce transitions within the degenerate subspace, in any order in perturbation theory. The transport properties of the system with $N \mod 4 = -1$ sites follow that of a nondegenerate ground state and the scattering matrix is given by $\mathcal{S} = \mathbb{1}_{4\times4}$.

To summarize the discussion above, it demonstrates that, at low voltage bias $eV \ll \Delta_g$, the interacting Majorana chain of length $2N$ is described by a unitary matrix. The form of the scattering matrix together with the ground-state degeneracy (or quantum dimension) allows us to fully resolve the fourfold periodicity of the chain. We note that the form of the scattering matrix for $\nu = 1$ and $\nu = 0$ depends exclusively on the possibility of a resonant single fermion tunneling and on the nondegeneracy of the ground state, respectively. As such, they are expected to persist for a general interaction profile of finite range and in the presence of generic local probes. The form of the scattering matrix is also remarkably generic for $\nu = 2$, since the time-reversal symmetry of the problem precludes tunnel-induced first order transitions within the degenerate ground state. Therefore, the transport properties measured in a two terminal setup can generically distinguish the presence or absence of a fermonic or spin-1/2-like zero modes, independent of the particular form of the interaction profile.

IV. THERMODYNAMIC LIMIT

Regarding the chain as the boundary of a stack of topological 1D superconductors, the distinct transport properties described above reflect the different nature of the zero modes localized at the boundary of the stacked system. In all of the three nontrivial classes the system hosts a topologically protected zero mode. This zero mode gives rise to a twofold degeneracy in the spectrum of the boundary. As this degeneracy is topologically protected, it must persist even when the boundary system is macroscopically large. The

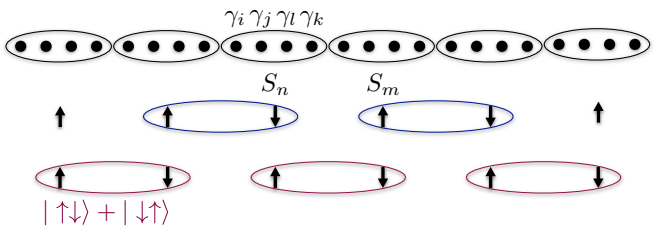

FIG. 4. An interacting Majorana chain, divided into groups of four per site. An intrasite interaction term couples the four Majorana modes leaving a twofold degeneracy per site corresponding to a spin-1/2 chain. Intersite interaction terms between two neighboring spins results in a unique spin-singlet ground state. The two ways in which the spin system can be coupled pairwise are topologically distinct.

trivial phase corresponding to $N \mod 4 = 0$, on the other hand, has a unique nondegenerate ground state for any finite N. This raises the question: which of these paradigms will reflect the characteristic behavior of the boundary system in the thermodynamic limit? A hint to the answer lies in the observation that while the degeneracy in the three nontrivial phases is protected by topology and *cannot* be lifted for any interaction profile, the nondegenerate ground state in the $N \mod 4 = 0$ case is a result of a *specific* (albeit generic) choice of the interaction Hamiltonian. (As a counterexample, a chain Hamiltonian with $N \mod 4 = 0$ and uniform all-to-all interactions is characterized by a twofold degenerate ground state.)

To address this question, it is instructive to consider a partition of the Majorana chain into sites consisting of four Majorana modes, as illustrated in Fig. 4. In the absence of interactions, the Majorana operators of each site span a fourfold degenerate ground state. An intrasite interaction term $\gamma_i\gamma_j\gamma_k\gamma_l$ couples the four Majorana modes leaving a twofold degeneracy per site. This, in fact, realizes a spin-1/2 chain. It can be readily verified that generic intersite interaction terms that couple two neighboring spins lift the fourfold degeneracy of their respective local Hilbert spaces resulting in a unique ground state of the two-spin system (Fig. 4). The two ways in which the local spins can be dimerized in pairs are topologically distinct, and the interface between them hosts a local spin-1/2 zero mode. We conclude by noting that the constant interaction profile chosen in our model lies at the phase boundary between these two distinct phases. It is therefore characterized by the presence of an extended (gapless) mode along the 1D chain. The energy of the extended mode scales inversely with the system size. In the thermodynamic limit, the excitation energy of this extended mode goes to zero and the ground state becomes doubly degenerate. This is indication of the emergence of a weak topological phase, namely a phase with an emergent zero mode protected by translational invariance. This is analogous to the emergent of a weak topological phase in a noninteracting model of stacked topological insulators [48]. This picture is supported by the scaling of the first excited state energy with system size (Fig. 2).

While the boundary zero mode remains stable for a generic interaction which does not break time-reversal and translational symmetry, its transport properties become progressively

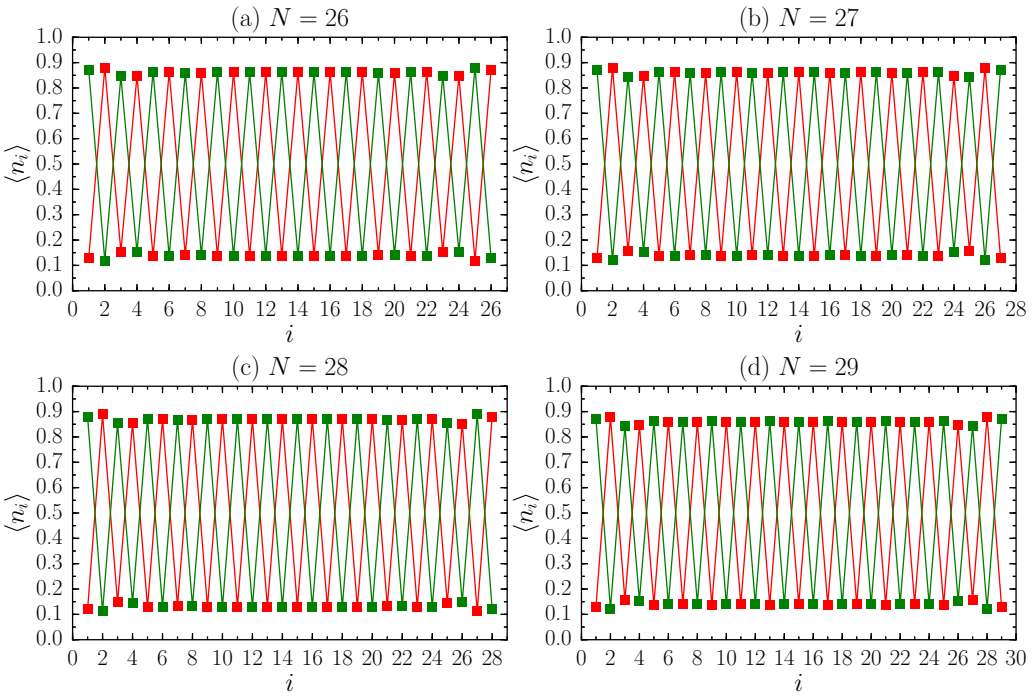

FIG. 5. The local density profile $\langle n_i \rangle = \langle \Psi_{1(2)} | d_i^\dagger d_i | \Psi_{1(2)} \rangle$ shown in green (red), respectively, for different system sizes ranging from $N = 26$ to $N = 29$. For $N = 26$, 27, and 29, $|\Psi_{1(2)}\rangle$ is the exactly twofold degenerate ground state. For $N = 28$, we use $|\Psi_{1(2)}\rangle = (|\tilde{\Psi}_1\rangle \pm |\tilde{\Psi}_2\rangle)/\sqrt{2}$, where $|\tilde{\Psi}_{1(2)}\rangle$ are the lowest two eigenstates of the Hamiltonian (1) separated by an energy splitting for finite-size chains. For each N, $|\Psi_{1(2)}\rangle$ form shifted charge density waves.

undetectable when the system is coupled to single channel leads. This is because the tunneling matrix element between the two degenerate ground states vanishes exponentially in this limit (Fig. 3). The reason for this exponential suppression can be seen in Fig. 5, which shows that the density profile of the two ground states form shifted charge density waves. Such a density profile indicates that the two ground states are expected to have exponentially vanishing matrix elements upon flipping the occupation locally at the system's end.

V. CONCLUSIONS

We have studied the transport properties of an interacting Majorana chain of length $2N$ with local interactions and coupled to external metallic leads. The model describes for example the low-energy excitations on the edge of stacked topological superconducting chains with a modified time-reversal symmetry. This stacked system falls into four topological classes depending on $N \mod 4$. We show that at low voltage bias, the transport properties of the 1D Majorana chain on the edge are characterized by a unitary scattering matrix, which, for finite but large N, partially reflects this fourfold periodicity. As a consequence the chain exhibits strikingly different transport properties for different $N \mod 4$. The four periodicity of the ground states can be fully identified by combining the transport properties with the quantum dimension of the system.

While the scattering properties along the Majorana chain are expected to depend on the detailed coupling to the leads and the form of interactions, the nature of the zero mode in the three nontrivial phases, is determined by topology. The results for a the gapped phase ($\nu = 0$), the fermionic zero-energy excitation ($\nu = 1$), and a spin-1/2-like excitation ($\nu = 2$) will remain the same for generic local probes, see discussion in Sec. III. Conversely, the results of the $\nu = 3$ phase is nongeneric and will depend on the detailed coupling to the even subchain or on breaking the subchain parity symmetries, and should be a subject of a separate detailed study.

We further provide numerical evidence that in the thermodynamic limit the chain has a twofold degenerate ground state. Regarding the Majorana chain as an effective model that emerges at the end of a system of stacked superconducting chains, the emergence of a robust mode indicates that the bulk two-dimensional system is in a weak interacting topological phase. Our finite-size numerics suggest that the two degenerate ground states form shifted charge density waves, indicating that the coupling to the leads vanishes exponentially with increasing system size. We note that while the transport characteristics along the Majorana chain of finite size are expected to depend on the detailed coupling to the leads and the form of interactions, the properties of the system in the thermodynamic limit do not, and the weak topological phase is robust for a generic interaction profile which does not break translational invariance.

ACKNOWLEDGMENTS

We acknowledge fruitful discussions in earlier stages of the work with Ehud Altman, Zohar Nussinov, Jonathan Ruhman, and Felix von Oppen. Z.L. was supported by the Alexander von

Humboldt Research Fellowship for Postdoctoral Researchers and the US Department of Energy, Office of Basic Energy Sciences through Grant No. DE-SC0002140. The latter was specifically for the use of computational facilities at Princeton University. E.J.B. was supported by the Wallenberg Academy Fellows program of the Knut and Alice Wallenberg Foundation. A.R. acknowledges support by EPSRC via Grant No. EP/P010180/1. D.M. acknowledges support from the Israel Science Foundation (Grant No. 737/14) and from the People Programme (Marie Curie Actions) of the European Union's Seventh Framework Programme (FP7/2007-2013) under REA Grant Agreement No. 631064.

APPENDIX: DERIVATION OF THE EFFECTIVE SD MODEL FOR $\nu = 2$

We perform a Schrieffer Wolff transformation on the Hamiltonian $H = H_0 + H_T$ [Eqs. (1) and (3)] taking into account virtual transitions to excited states. For this purpose we define the following projection operators on the ground-state manifold and on the excited states, respectively:

$$\mathcal{P}_g = |\mathrm{gs}_{+-}\rangle\langle \mathrm{gs}_{+-}| + |\mathrm{gs}_{-+}\rangle\langle \mathrm{gs}_{-+}|,$$
$$\mathcal{P}_e = 1 - \mathcal{P} = \sum_{n,s,s'} |n_{s,s'}\rangle\langle n_{s,s'}|,$$

where the sum is over excited states $|n_{s,s'}\rangle$, for which $H_0|n_{s,s'}\rangle = E_n|n_{s,s'}\rangle$, $P_o|n_{s,s'}\rangle = s|n_{s,s'}\rangle$, and $P_e|n_{s,s'}\rangle = s'|n_{s,s'}\rangle$. Noting that tunneling events from the right lead change the parity on the even subchain while tunneling events on the left lead change the parity of the odd subchain, the matrix elements of the tunneling Hamiltonian between the ground-state manifold and excited states are

$$H_{ge} = \mathcal{P}_g H \mathcal{P}_e = \mathcal{P}_g H_T \mathcal{P}_e = \sum_k \sum_n \{|\mathrm{gs}_{+-}\rangle\langle n_{++}|(t_R c^\dagger_{R,k}\tilde{\beta}_n + t^*_R c_{R,k}\tilde{\alpha}^*_n) + |\mathrm{gs}_{+-}\rangle\langle n_{--}|(t_L c^\dagger_{L,k}\beta_n - t^*_L c_{L,k}\alpha^*_n)$$
$$+ |\mathrm{gs}_{-+}\rangle\langle n_{++}|(t_L c^\dagger_{L,k}\alpha_n - t^*_L c_{L,k}\beta^*_n) + |\mathrm{gs}_{-+}\rangle\langle n_{--}|(t_R c^\dagger_{R,k}\tilde{\alpha}_n + t^*_R c_{R,k}\tilde{\beta}^*_n)\},$$

where we have used the relations which follow from charge conjugation symmetry T_L:

$$\alpha_n = \langle \mathrm{gs}_{-+}|d_1|n_{++}\rangle = (\langle \mathrm{gs}_{+-}|d^\dagger_1|n_{--}\rangle)^*,$$
$$\beta_n = \langle \mathrm{gs}_{+-}|d_1|n_{--}\rangle = (\langle \mathrm{gs}_{-+}|d^\dagger_1|n_{++}\rangle)^*,$$
$$\tilde{\alpha}_n = \langle \mathrm{gs}_{-+}|d_N|n_{--}\rangle = -(\langle \mathrm{gs}_{+-}|d^\dagger_N|n_{++}\rangle)^*,$$
$$\tilde{\beta}_n = \langle \mathrm{gs}_{+-}|d_N|n_{++}\rangle = -(\langle \mathrm{gs}_{-+}|d^\dagger_N|n_{--}\rangle)^*.$$

The resulting effective model is given by $H_{\mathrm{eff}} = H_{ge}(E_g - H_{ee})^{-1}H_{eg}$:

$$H_{\mathrm{eff}} = |\mathrm{gs}_{+-}\rangle\langle \mathrm{gs}_{+-}| \sum_{k,k'}\sum_n \left\{|t_R|^2\frac{|\tilde{\beta}_n|^2 - |\tilde{\alpha}_n|^2}{E_g - E_n}c^\dagger_{R,k}c_{R,k'} + |t_L|^2\frac{|\beta_n|^2 - |\alpha_n|^2}{E_g - E_n}c^\dagger_{L,k}c_{L,k'} + \left(|t_R|^2\frac{|\tilde{\alpha}_n|^2}{E_g - E_n} + |t_L|^2\frac{|\alpha_n|^2}{E_g - E_n}\right)\delta_{k,k'}\right\}$$
$$+ |\mathrm{gs}_{-+}\rangle\langle \mathrm{gs}_{-+}| \sum_{k,k'}\sum_n \left\{|t_R|^2\frac{|\tilde{\alpha}_n|^2 - |\tilde{\beta}_n|^2}{E_g - E_n}c^\dagger_{R,k}c_{R,k'} + |t_L|^2\frac{|\alpha_n|^2 - |\beta_n|^2}{E_g - E_n}c^\dagger_{L,k}c_{L,k'} + \left(|t_R|^2\frac{|\tilde{\beta}_n|^2}{E_g - E_n} + |t_L|^2\frac{|\beta_n|^2}{E_g - E_n}\right)\delta_{k,k'}\right\}$$
$$+ |\mathrm{gs}_{+-}\rangle\langle \mathrm{gs}_{-+}| \sum_{k,k'}\sum_n \left(t_R t^*_L\frac{2\tilde{\beta}_n\alpha^*_n}{E_g - E_n}c^\dagger_{R,k}c_{L,k'} + t_R t_L\frac{2\tilde{\beta}_n\beta_n}{E_g - E_n}c^\dagger_{L,k}c^\dagger_{R,k'} + t^*_R t^*_L\frac{2\tilde{\alpha}^*_n\alpha^*_n}{E_g - E_n}c_{R,k}c_{L,k'} + t^*_R t_L\frac{2\tilde{\alpha}^*_n\beta_n}{E_g - E_n}c^\dagger_{L,k}c_{R,k'}\right)$$
$$+ \mathrm{H.c.}$$
$$= \tau_z \sum_{k,k'}\sum_n \left\{|t_R|^2\frac{|\tilde{\beta}_n|^2 - |\tilde{\alpha}_n|^2}{E_g - E_n}c^\dagger_{R,k}c_{R,k'} + |t_L|^2\frac{|\beta_n|^2 - |\alpha_n|^2}{E_g - E_n}c^\dagger_{L,k}c_{L,k'} - \frac{\delta_{k,k'}}{2}\left(|t_R|^2\frac{|\tilde{\beta}_n|^2 - |\tilde{\alpha}_n|^2}{E_g - E_n} + |t_L|^2\frac{|\beta_n|^2 - |\alpha_n|^2}{E_g - E_n}\right)\right\}$$
$$+ \left\{\tau_+ \sum_{k,k'}\sum_n \left(t_R t^*_L\frac{2\tilde{\beta}_n\alpha^*_n}{E_g - E_n}c^\dagger_{R,k}c_{L,k'} + t_R t_L\frac{2\tilde{\beta}_n\beta_n}{E_g - E_n}c^\dagger_{L,k}c^\dagger_{R,k'} + t^*_R t^*_L\frac{2\tilde{\alpha}^*_n\alpha^*_n}{E_g - E_n}c_{R,k}c_{L,k'} + t^*_R t_L\frac{2\tilde{\alpha}^*_n\beta_n}{E_g - E_n}c^\dagger_{L,k}c_{R,k'}\right) + \mathrm{H.c.}\right\},$$

where the last equation is up to an additive constant and we have defined $\tau_z = |\mathrm{gs}_{+-}\rangle\langle \mathrm{gs}_{+-}| - |\mathrm{gs}_{-+}\rangle\langle \mathrm{gs}_{-+}|$ and $\tau_+ = |\mathrm{gs}_{+-}\rangle\langle \mathrm{gs}_{-+}|$. Introducing the coefficients:

$$J_z = \sum_n \left\{|t_R|^2\frac{|\tilde{\beta}_n|^2 - |\tilde{\alpha}_n|^2}{E_g - E_n} - |t_L|^2\frac{|\beta_n|^2 - |\alpha_n|^2}{E_g - E_n}\right\},$$
$$J_- = 2t_R t^*_L \sum_n \frac{\tilde{\beta}_n\alpha^*_n}{E_g - E_n}, \quad J_+ = 2t^*_R t_L \sum_n \frac{\tilde{\alpha}^*_n\beta_n}{E_g - E_n},$$

and

$$\Delta_z = \sum_n \left\{ |t_R|^2 \frac{|\tilde{\beta}_n|^2 - |\tilde{\alpha}_n|^2}{E_g - E_n} + |t_L|^2 \frac{|\beta_n|^2 - |\alpha_n|^2}{E_g - E_n} \right\},$$

$$\Delta_+ = 2t_R t_L \sum_n \frac{\tilde{\beta}_n \beta_n}{E_g - E_n}, \quad \Delta_- = 2t_R^* t_L^* \sum_n \frac{\tilde{\alpha}_n^* \alpha_n^*}{E_g - E_n},$$

we arrive at the expression given in Eq. (9) of the main text.

[1] A. Rahmani, X. Zhu, M. Franz, and I. Affleck, Phys. Rev. Lett. **115**, 166401 (2015).
[2] S. Sachdev and J. Ye, Phys. Rev. Lett. **70**, 3339 (1993).
[3] A. Kitaev, http://online.kitp.ucsb.edu/online/entangled15/kitaev/, http://online.kitp.ucsb.edu/online/entangled15/ kitaev2/ (2015).
[4] J. Maldacena and D. Stanford, Phys. Rev. D **94**, 106002 (2016).
[5] A. Jevicki and K. Suzuki, J. High Energy Phys. **11** (2016) 046.
[6] Y.-Z. You, A. W. W. Ludwig, and C. Xu, Phys. Rev. B **95**, 115150 (2017).
[7] S. Banerjee and E. Altman, Phys. Rev. B **95**, 134302 (2017).
[8] J. S. Cotler, G. Gur-Ari, M. Hanada, J. Polchinski, P. Saad, S. H. Shenker, D. Stanford, A. Streicher, and M. Tezuka, J. High Energy Phys. **05** (2017) 118.
[9] R. A. Davison, W. Fu, A. Georges, Y. Gu, K. Jensen, and S. Sachdev, Phys. Rev. B **95**, 155131 (2017).
[10] K. Jensen, Phys. Rev. Lett. **117**, 111601 (2016).
[11] Y. Gu, X.-L. Qi, and D. Stanford, J. High Energy Phys. **05** (2017) 125.
[12] D. I. Pikulin and M. Franz, Phys. Rev. X **7**, 031006 (2017).
[13] E. Witten, arXiv:1610.09758.
[14] D. J. Gross and V. Rosenhaus, J. High Energy Phys. **02** (2017) 093.
[15] I. Affleck, A. Rahmani, and D. Pikulin, Phys. Rev. B **96**, 125121 (2017).
[16] A. Chew, A. Essin, and J. Alicea, Phys. Rev. B **96**, 121119(R) (2017).
[17] A. Milsted, L. Seabra, I. C. Fulga, C. W. J. Beenakker, and E. Cobanera, Phys. Rev. B **92**, 085139 (2015).
[18] A. Rahmani, X. Zhu, M. Franz, and I. Affleck, Phys. Rev. B **92**, 235123 (2015).
[19] L. Fidkowski and A. Kitaev, Phys. Rev. B **81**, 134509 (2010).
[20] L. Fidkowski and A. Kitaev, Phys. Rev. B **83**, 075103 (2011).
[21] A. M. Turner, F. Pollmann, and E. Berg, Phys. Rev. B **83**, 075102 (2011).
[22] V. Gurarie, Phys. Rev. B **83**, 085426 (2011).
[23] T. Morimoto, A. Furusaki, and C. Mudry, Phys. Rev. B **92**, 125104 (2015).
[24] A. Kitaev, Physics-Uspekhi **44**, 16 (2001).
[25] J. Alicea, Reports Prog. Phys. **75**, 76501 (2012).
[26] C. W. J. Beenakker, Rev. Mod. Phys. **87**, 1037 (2015).
[27] I. C. Fulga, F. Hassler, A. R. Akhmerov, and C. W. J. Beenakker, Phys. Rev. B **83**, 155429 (2011).
[28] I. C. Fulga, F. Hassler, and A. R. Akhmerov, Phys. Rev. B **85**, 165409 (2012).
[29] M.-T. Rieder, P. W. Brouwer, and İ. Adagideli, Phys. Rev. B **88**, 060509(R) (2013).
[30] V. Mourik, K. Zuo, S. M. Frolov, S. R. Plissard, E. P. A. M. Bakkers, and L. P. Kouwenhoven, Science **336**, 1003 (2012).
[31] A. Das, Y. Ronen, Y. Most, Y. Oreg, M. Heiblum, and H. Shtrikman, Nat. Phys. **8**, 887 (2012).
[32] S. Nadj-Perge, I. K. Drozdov, J. Li, H. Chen, S. Jeon, J. Seo, A. H. MacDonald, B. A. Bernevig, and A. Yazdani, Science **346**, 602 (2014).
[33] M. T. Deng, S. Vaitiekėnas, E. B. Hansen, J. Danon, M. Leijnse, K. Flensberg, J. Nygård, P. Krogstrup, and C. M. Marcus, Science **354**, 1557 (2016).
[34] D. Meidan, A. Romito, and P. W. Brouwer, Phys. Rev. Lett. **113**, 057003 (2014).
[35] D. Meidan, A. Romito, and P. W. Brouwer, Phys. Rev. B **93**, 125433 (2016).
[36] In this context the quantum dimension is defined as the ground-state degeneracy.
[37] A. Altland and M. R. Zirnbauer, Phys. Rev. B **55**, 1142 (1997).
[38] A. Kitaev, V. Lebedev, and M. Feigelman, AIP Conf. Proc. **1134**, 22 (2009).
[39] A. P. Schnyder, S. Ryu, A. Furusaki, and A. W. W. Ludwig, Phys. Rev. B **78**, 195125 (2008).
[40] L. Fidkowski, R. M. Lutchyn, C. Nayak, and M. P. A. Fisher, Phys. Rev. B **84**, 195436 (2011).
[41] G. E. Blonder, M. Tinkham, and T. M. Klapwijk, Phys. Rev. B **25**, 4515 (1982).
[42] Y. Blanter and M. Büttiker, Phys. Rep. **336**, 1 (2000).
[43] M. P. Anantram and S. Datta, Phys. Rev. B **53**, 16390 (1996).
[44] P. Coleman and A. J. Schofield, Phys. Rev. Lett. **75**, 2184 (1995).
[45] P. Coleman, L. B. Ioffe, and A. M. Tsvelik, Phys. Rev. B **52**, 6611 (1995).
[46] T. K. Ng and P. A. Lee, Phys. Rev. Lett. **61**, 1768 (1988).
[47] The negative values of ν can be understood as follows. For a noninteracting chain of Majorana fermions with time-reversal symmetry $T^2 = 1$, the Majorana zero modes can be classified as even or odd under the action of time-reversal symmetry according to $T\gamma_j T^{-1} = \pm\gamma_j$. In a noninteracting chain hosting both even and odd Majorana zero modes, quadratic coupling terms pairing Majoranas with different parity are allowed, and the topological index $\nu \in \mathbb{Z} = N_e - N_o$ is given by the number of unpaired Majorana zero modes. Here $\nu < 0$ stands for $N_o = \nu$ odd Majorana modes. In this representation, the eight distinct topological phases are given by $\nu \in [-3,4]$. For chains with $2N$ Majorana modes considered here, this yields N mod $4 \in [-1,2]$, and the $\nu = 3$ case is consistently identified with the $\nu = -1$.
[48] Z. Ringel, Y. E. Kraus, and A. Stern, Phys. Rev. B **86**, 045102 (2012).